ORIGINAL ARTICLE

Titania Nanotube Arrays Nanosystem for Therapeutic Delivery of Resveratrol on Neuronal Cell lines Model

Wan Nuramiera Faznie Wan Eddis Effendy[1], Rabiatul Basria S. M. N. Mydin[1,2], Srimala Sreekantan[3], Syafiqa Farhana Ahmad Sopian[4], Priya Sundaraju[5], Sharenia Gunasagaran[5], Amirah Mohd Gazzali[6]

[1] Oncological and Radiological Sciences Cluster, Advanced Medical and Dental Institute, Universiti Sains Malaysia, Bertam Kepala Batas 13200, Pulau Pinang, Malaysia.
[2] Department of Biological Sciences, National University of Singapore, 14 Science Drive 4, 117543 Singapore.
[3] School of Materials and Mineral Resources Engineering, Engineering Campus, Universiti Sains Malaysia, Nibong Tebal 14300, Penang, Malaysia.
[4] Faculty of Applied Sciences, Universiti Teknologi MARA (UiTM), Arau 02600, Perlis, Malaysia.
[5] Faculty of Science and Mathematics, Sultan Idris Education University, Tanjung Malim, Perak 35900, Malaysia.
[6] School of Pharmaceutical Sciences, Universiti Sains Malaysia, Gelugor 11800, Penang, Malaysia.

ABSTRACT

Introduction: The therapeutic delivery nanosystem attracts major interest due to its potential in improving the effectiveness and minimising the drawback of treatments especially in the neuroscience field. This work investigates the potential of the titania nanotube arrays (TNA) nanosystem as the therapeutic delivery for resveratrol (RSV) to the neuronal cell line model. **Methods:** TNA was fabricated using electrochemical anodisation in an organic electrolyte, and the morphology of the nanotube structure was analysed using field-emission scanning electron microscopy. The dose-dependent study of SH-SY5Y cell lines was conducted by testing different concentrations of RSV for 24 h by using the tetrazolium inner salt (MTS reagent). The RSV release profile of the chitosan-coated TNA nanosystem was characterised in the biphasic condition of the sample immersed in phosphate-buffered saline at 37 °C. Subsequently, the functional analysis of RSV release from the TNA nanosystem by using an *in-vitro* cell culture model was characterised on the neuronal cell line model SH-SY5Y for 48 and 72 h. **Results:** Within the first 6 h and after 14 d, 23.41% ± 13.12% and approximately 49.01% ± 9.74%, respectively, of RSV were released from the chitosan-coated TNA nanosystem. SH-SY5Y cells were inhibited when cells were incubated in uncoated and chitosan-coated RSV-loaded TNA, thereby displaying the potential of TNA to load and release RSV in the *in-vitro* culture system. **Conclusion:** The findings from this study highlight the potential of TNA nanosystems to overcome the limitation in the delivery of the therapeutic compound especially in the neuroscience field.

Keywords: Titania nanotube arrays nanosystem, Resveratrol-loaded nanosystem, Therapeutic delivery compound, Neuronal cell line model

Corresponding Author:
Rabiatul Basria S.M.N Mydin, PhD
Email: rabiatulbasria@usm.my
Tel: +604-5622351

INTRODUCTION

The therapeutic delivery of nanomaterials in treating neurological disorders has been reported to aid in the penetration of the drug to the blood–brain barrier (BBB) and the central nervous system barriers (1, 2). Some of the nanomaterials used before are TiO_2 nanoparticles (NP) due to its excellent biocompatibility and reduced toxicity properties (3). However, the free-form NP has become a disadvantage when passing these barriers, resulting in neurotoxicity and neurodegeneration caused by the accumulated NP (4). Moreover, genetic toxicity *ex vivo* is highlighted as a drawback on the uses of TiO_2 NP in a dose-dependent manner (5). Hence, this study suggests another alternative to overcome this concern and fully exploit the unique characteristics of TiO_2 for biomedical application.

The titania nanotube arrays (TNA) is designed to increase the potential of this material in biomedical application and overcome the above concern. Generally, TNA exhibits additional characteristics compared with TiO_2 NP. TNA can promote cell attachment, adhesion and proliferation and has a low corrosion rate and high surface area per volume, which help in the loading of various compounds, such as antimicrobials, genes, proteins and drugs (6 – 8). In this work, the natural compound resveratrol (RSV) is loaded into the TNA nanocomplex for drug delivery application for neuroblastoma cell (SH-SY5Y) targeting. This cell line is chosen due to its similar characteristics to the neuron cell and widely studied in

neurology-related diseases (9, 10).

RSV, a polyphenolic compound, is a well-known therapeutic material in neuroscience application. As a neuroprotective agent, RSV can promote neuroregeneration especially in severe brain injury (11). Several studies have reported the ability of this compound to promote cell proliferation and cell function and prevent neuronal cell death (12-14). This compound presents various benefits but has low solubility and stability, which may be improved by loading into TNA and coating with the chitosan biopolymer.

The chitosan biopolymer manifests higher hydrophilic properties and water vapor permeability compared with the polylactic acid polymer (15, 16). In addition, the co-micellar system possesses hydrophobic and hydrophilic properties (17) and may degrade and enter the BBB, leading to brain cell damage. Therefore, the chitosan biopolymer is an ideal coating material for this nanocomplex application. Other than these two properties, the chitosan biopolymer exhibits antimicrobial, good degradability and high swelling properties (18). However, the application of the chitosan-coated TNA–RSV nanocomplex in brain studies has not been reported yet although RSV has noticeable properties in protecting and improving the injury of neuron cells. This work is conducted to improve the TNA nanosystem for therapeutic compound targeting the neuroblastoma cell line.

MATERIALS AND METHODS

Electrochemical anodisation of TNA and FESEM characterisation

TNA fabrication was performed according to previously reported method by Mydin et al, 2017. Surface morphology of TNA before and after biopolymer coating was analysed by FESEM, Supra 35 VP Zeiss, Germany without gold coating method as for re-use purposes for *in-vitro* work after FESEM observation. The magnification was standardised at 100 kX magnification at frequency 15 kHz. Energy dispersive X-ray (EDX) was analysed by INCA Microanalysis Suite software with magnification 10 kX.

Therapeutic compound preparation and quantification

Resveratrol (Tokyo Chemical Industry Co Ltd, America) was prepared in ethanol (50 mg/mL) for stock (500 µM) and stored at 4 °C as stated by Buhrmann et al, 2019. Quantification of RSV was performed by direct spectrophotometric measurement at 320 nm. Detection of absorbance against serial RSV dilution was plotted as reference for RSV quantification in therapeutic release profile study.

Cell culture treatment

Neuroblastoma SH-SY5Y cell line model (ATCC® CRL-2266™) was cultured in complete DMEM (Gibco, Life Technologies) medium (10 % (v/v) fetal bovine serum (FBS), 2 g/L sodium bicarbonate, 12.5 mg/L HEPES, 5 % (v/v) L-glutamine and 1% (v/v) penicillin and streptomycin) at 37 °C in a 5 % CO2 humidified incubator. Assessment of cell viability was performed after 24, 48 and 72 h treatment by CellTiter 96®AQueous One Solution Cell Proliferation Assay (Promega, USA) according to the manufacturer's protocol at 490 nm using microplate spectrophotometer reader (PowerWave™ BioTek, USA). The determination of half maximal inhibitory concentration (IC_{50}) was performed following the protocol recommendations in ISO 10993-5.

Resveratrol loading into TNA

TNA samples with measurement 1 cm x 1 cm were sterilised and placed in individual container containing 100 µM of RSV for 24 h at 4 °C follow by 2 h air-dried before polymer coating procedure (21).

Chitosan coating preparation

Chitosan (low molecular weight, Sigma Aldrich, St. Louis, USA) was diluted in 1 % (v/v) acetic acid with continuous shaking at 60 °C for 5 h using incubator shaker (KS 4000i Control, Germany). The study samples coated with this solution by one-time dip coating technique as described by Liang et al, 2018 and air-dried under biosafety cabinet level 2 for overnight.

Resveratrol release profile from TNA nanosystem

RSV-loaded TNAs (coated and uncoated samples) were immersed in PBS and incubated at 37 °C with continuous shaking at 100 rpm. RSV quantification were studied at two phases: burst release for every 30 mins (6 h) and prolonged release in 14 d described by Kumeria et al, 2015.

Statistical analysis

Data are expressed as mean ± SD for at least two or three experiments. Data on *in-vitro* drug release was statistically analysed by two-way ANOVA test, while paired student T-test was applied for other result in which *p* value lower than 0.05 was considered significant.

RESULTS

Topological analysis of the chitosan coating of the RSV-loaded TNA

The anodisation curve of TNA in organic electrolyte (i.e. glycerol) is displayed in Fig. 1. TNA with average diameter of around 60–90 nm was successfully fabricated from electrochemical anodisation at 30 V and 30 mins (Fig. 2 (a)). The outcome of the electrochemical anodisation was similar as those reported in previous works (24, 25). The EDX analysis displayed in Fig. 2 (b) presented Ti and O elements on the surface, indicating the formation of TNA through electrochemical anodisation. Wang et al. (2018) have described TNA with diameter between 30 and 100 nm, which is the most desirable measurement for drug loading and cell attachment. In the present

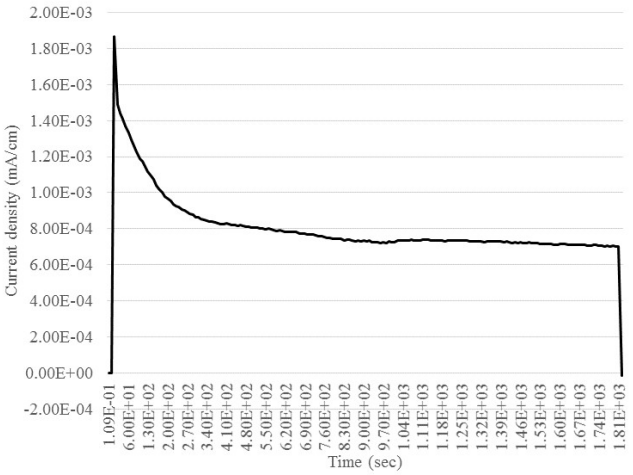

Figure 1: Anodisation curve of titania nanotube array (TNA) by electrochemical anodisation in organic solvent at 30 V, 30 mins.

study, the topology comparison of the chitosan coating of RSV-loaded TNA before and after release is shown in Figs. 2 (c) and 2 (d). Fig. 2 (c) displays a fully covered TNA with chitosan from the one-time dip coating layer. The TNA nanosurface acts as reservoir for RSV, and the chitosan coating layer serves as a protective layer for RSV-loaded TNA. Further topological observation on chitosan-coated TNA after the 14 d RSV release study is shown in Fig. 2 (d). About 35% of chitosan traces are still observed after this release period. This observation can explain the low detection of RVS throughout the study, suggesting that a long release study should be conducted to achieve the maximum release of RSV.

Standard Curve of RSV release from the chitosan-coated TNA

The RSV release was detected at specific wavelength (320 nm) by using spectrophotometry (27, 28). The initial direct absorbance measurement was performed using varying concentrations of RSV starting at 1000 µM, as shown in Fig. 3.

RSV cytotoxicity profile on the SH-SY5Y cell line model

The neuroblastoma cell line SH-SY5Y is commonly used in the study of brain disorders and acts as model for neuronal cell line (29, 30). The microscopic observation of the SH-SY5Y cell (Fig. 4) demonstrated changes in cell number and morphology after treatment with RSV at different dilutions. Compared with the untreated cell (a), the cell that underwent treatment had changes in cell morphology (g, h, i) and shrank (c - i) at 0.28 - 20 µM. This outcome was expected because Van Ginkel and co-workers have reported that RSV can inhibit the growth of SH-SY5Y cell lines.

The IC_{50} value, the baseline value in evaluating the optimum dose of RSV to be loaded into TNA for the

a

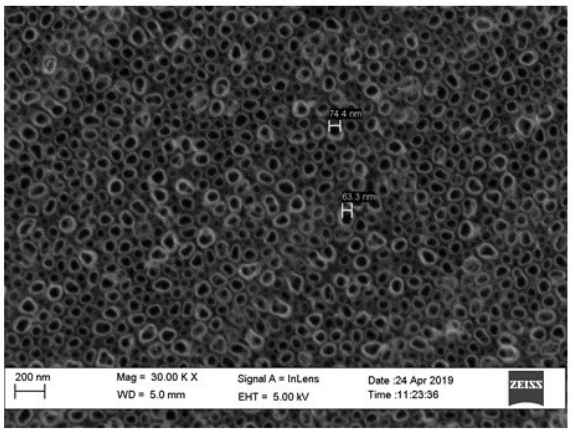

b

Element	Weight%	Atomic%
C K	0.74	1.59
O K	33.48	53.82
F K	11.36	15.37
Ti K	54.42	29.22
Totals	100.00	

c

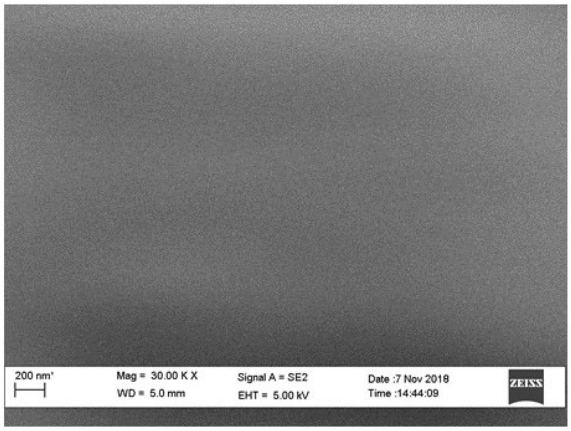

d

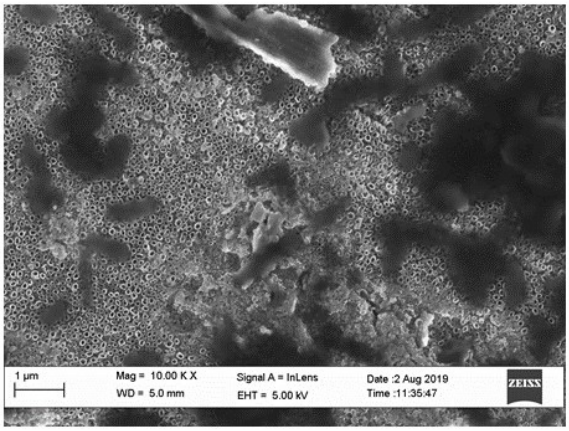

Figure 2: Topological images of the chitosan coating on titania nanotube arrays (TNA) before and after RSV release obtained using field-emission scanning electron microscope: (a) Naked observation of TNA without any surface modification, (b) EDX analysis of fabricated TNA, (c) chitosan coating of RSV-loaded TNA, and (d) chitosan-coated TNA after the 14 d RSV release study.

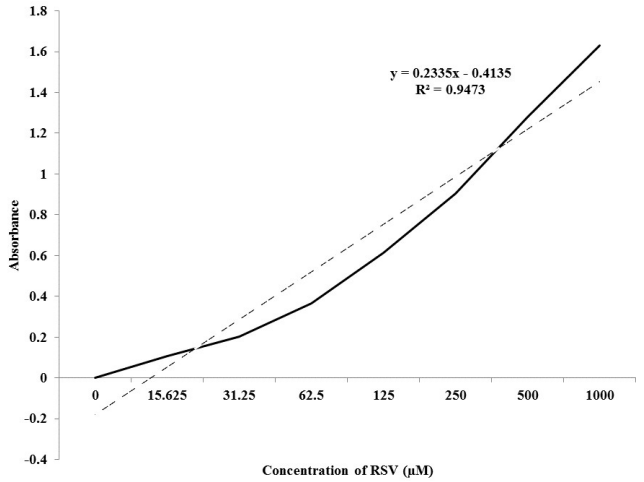

Figure 3: RSV standard curve used for RSV release calculation from chitosan-coated TNA through direct spectrophotometric measurement. The positive linear relationship of RSV absorbance and concentration was observed at 320 nm for reference calculation in the RSV release profile.

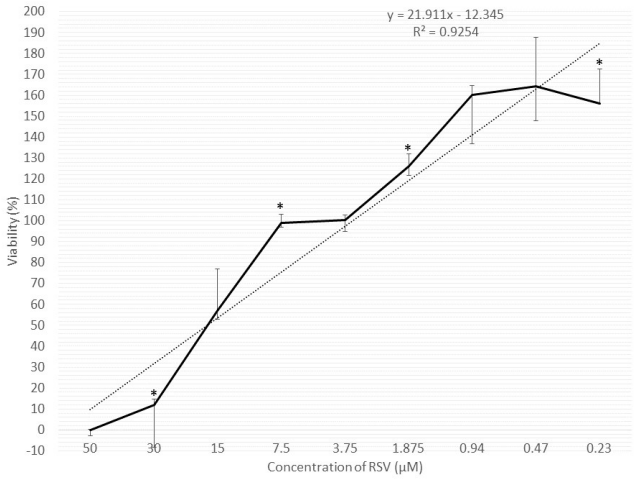

Figure 5: Cell viability assay of SH-SY5Y cell lines on different concentrations of RSV for 24 h. All data were normalised using untreated data as control in this study. Tests were conducted in triplicate, and data were expressed as mean ± SD. Data with asterisk showed significant difference between sample and untreated sample.

therapeutic release activity on the studied cell, was 8.29 µM. The proliferation of SH-SY5Y was inversely proportional to the dose as lower dose of RSV increased the cell viability while the cell viability decreased when the cell was exposed to higher concentration. The lowest dose that caused increased cell viability was observed at 0.23 µM of RSV, as demonstrated in Fig. 5. By contrast, increasing the concentration of RSV from 3.75 µM to 30.00 µM decreased the cell viability (Fig. 5). Above 50.00 µM, the SH-SY5Y was totally inhibited, which was similar to the phenomenon known as the double-edged sword of RSV reported by Salehi and co-workers.

Release profile of RSV from TNA

The RSV release profile from chitosan-coated TNA for 14 d (Fig. 6) was studied and compared with the *in-vitro* findings in Fig. 7. A total of 50 µM was loaded into both samples by using the immersion method. The concentration of loaded RSV was higher than the IC_{50} value from the cytotoxicity testing because we expected a slow release of RSV from TNA based on the literature (33, 34).

From the release profile in Figs. 6 (a, b), the RSV-loaded

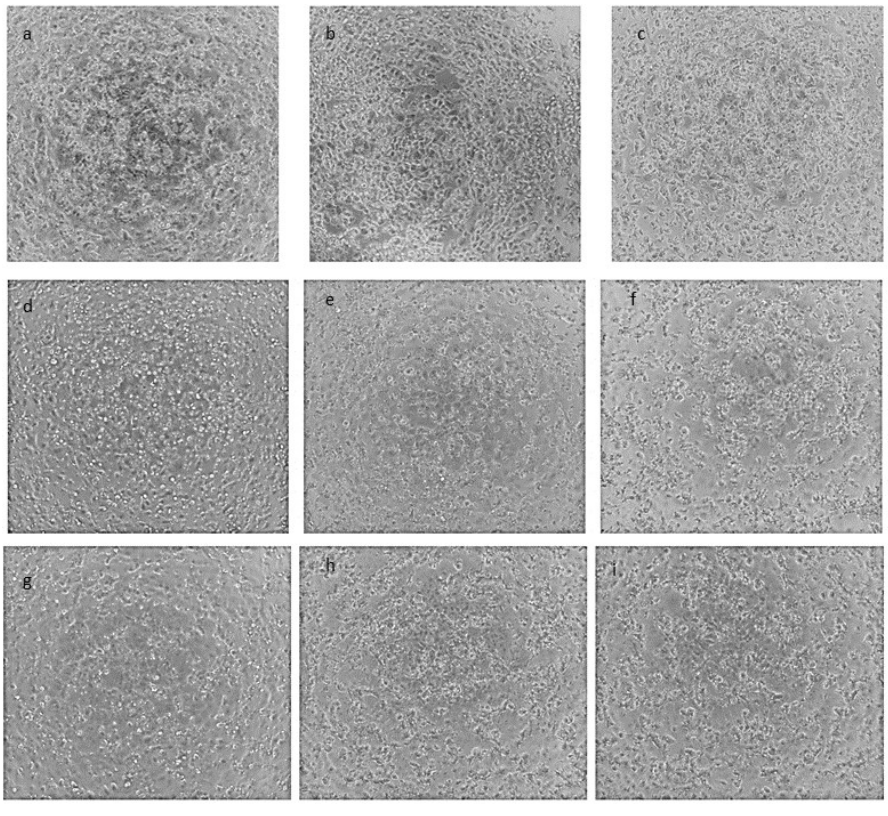

Figure 4: Morphological analysis of SH-SY5Y cell lines after 24 h incubation with different concentration of RSV at 10k magnification.

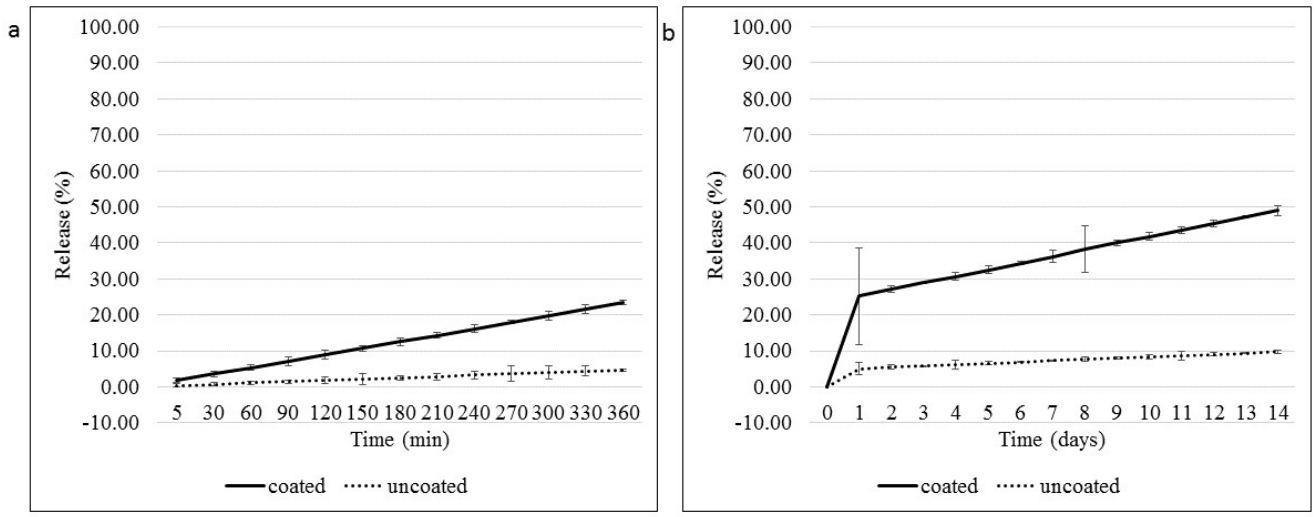

Figure 6: RSV release profile from chitosan-coated TNA for 14 d in the PBS system. (a) Burst release profile of coated and uncoated RSV-loaded into TNA studied during the first 6 h interaction of sample in the PBS solution. (b) The release profile was determined for 14-d, and data were recorded daily. All data were expressed as mean (n = 4).

TNA (coated) recorded higher release compared with the uncoated RSV-loaded TNA for both phases, which could be caused by the swelling of chitosan that forced the release of RSV (35). The burst release study showed 23.41% ± 13.12% release from the coated sample and 5.67% ± 2.36% release from the uncoated sample, and the paired student T-test showed that these values were not significantly different (p = 1.000). At prolonged release (days 1 to 14), the coated sample displayed more than 49.01% ± 9.74% release, whereas the uncoated sample only released around 9.74% ± 0.4% throughout the study.

No significant difference was observed between the cell viability of SHSY-5Y and all samples tested for 24 h in the time-dependent testing (p value = 0.216). As such, the 48 and 72 h incubation periods were used in the subsequent tests, which was in line with the aim of the study of demonstrating prolonged and continuous release of RSV in the *in-vitro* study. The two-way ANOVA statistical analysis was used to analyse the SH-SY5Y viability as there were two group; time (48 and 72 h) and different type of TNA nanocomplexes tested. The data showed normal distribution from the Shapiro–Wilk test (p > 0.05) except for data of cell treated with RSV alone (p = 0.000) hence fulfil the requirement for this test to be applied in this work.

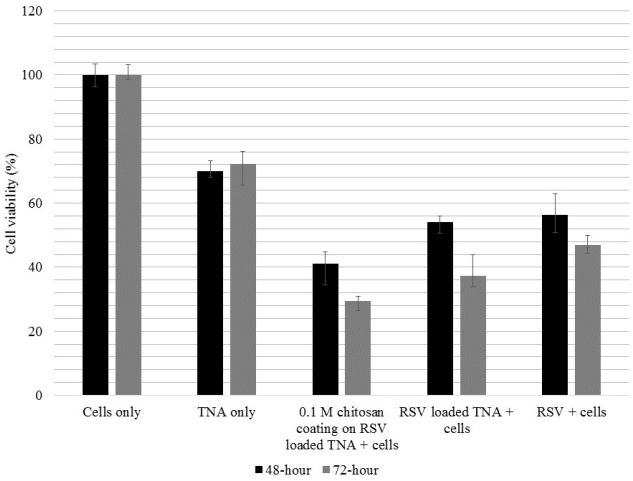

Figure 7: Comparison of RSV-loaded TNA coated and uncoated with chitosan. Cell viability after treatment was presented in two incubation periods (48 and 72 h). Experiments were carried out in quadruplicate (n = 4), and the data were analysed in mean ± SD. No significant difference was observed in chitosan-coated and uncoated RSV-loaded TNA.

Generally, the data from 48 and 72 h incubation period showed no significant difference (p = 0.152). The viability of the SH-SY5Y cells after interaction with different samples was significantly different (p = 0.0001) from that of the cells incubated only for 48 and 72 h. However, the RSV alone and the RSV-loaded TNA had no significant difference in terms of cell inhibition, suggesting that the decreased cell viability was caused by RSV alone and not caused by stress from the TNA sample. Thus, this finding supported the unique characteristics of TNA as highly biocompatible for biomedical implant (Hazan et al, 2016). No significant difference (p = 0.119) was also observed between samples of RSV-loaded TNA and chitosan-coated RSV-loaded TNA. TNA and chitosan coating were believed to not influence the cell viability when introduced into the cell culture medium and incubated for a certain period (Fig. 7).

The Pearson's correlation analysis (–0.718) showed a negative relationship between the period of study and the cell viability at two periods, indicating that prolonged period lowered the cell viability. This finding was in line with our objective, in which longer exposure to the drug-loaded TNA sample increased cell death constantly until all drugs had been released.

DISCUSSION

The positive relationship of the RSV concentration and

absorbance is obtained, indicating the RSV release profiles. Tosato et al. (2018) have described influence on the uses of ethanolic solvent in RSV detection at a wavelength ranging from 300 nm to 360 nm. It had been discussed that due to the trans and the cis forms of the RSV, dilution of the compound with ethanolic solvent was suitable and not harmful to cells especially at low concentration. Thus, the direct detection of RSV at 320 nm was suitable for drug release profile study and applied throughout this study.

Arbo and co-workers have described the neuroprotective properties of RSV, which agree with our findings in Fig. 5. The low concentration of RSV can promote the cell proliferation, which shown an increased in the cell viability for about 1.4 times at 0.23 µM. Therefore, the determination of the optimum concentration of RSV to be loaded into TNA plays an important role in increasing cell proliferation or inhibiting cell viability. In the therapeutic release investigation, a high dose of RSV is loaded to inhibit the growth of the abnormal neuron cell, which is mostly found in neurological disorders, such as brain cancer, Parkinson's disease and Alzheimer's disease (39). Neurons contain a protective barrier, which interferes with the conventional treatment. Thus, nanotherapeutics may be an alternative in the future.

Another study has shown that the release pattern of the uncoated sample is usually higher than that of the coated sample, which is different from our work. Moreover, in contrast to our study, the previous study has demonstrated that the coated samples are effective in decreasing the cell viability (Fig. 7), which is similar to the RSV release shown in Figs. 6 (a) and 7 (b). This finding is supported by the report of Hanif et al. (2016) that states that the time required for RSV to release from the nanotube structure is 48 h. In the same report, halloysite nanotubes, which are hydrophobic, are studied because they protect and stabilise the RSV compound. Other study shown that the naked TNA and resveratrol presented with hydrophobic characteristics while on the other hands, chitosan is a hydrophilic compound. This combination will make the nanocomplex favourable in water-like condition with first layer chitosan will be degraded before releasing of RSV took place. Therefore, the stability of RSV might be maintained until reached the targeted site, however more studies still need to be conducted to understand the mechanism involved.

The inhibitory effect of RSV at higher dose indicates the effective loading and release of the therapeutic compound from TNA into the SH-SY5Y. The implementation of the chitosan coating can prevent the degradation and prolong the release of RSV upon contact with the culture medium *in-vitro*. RSV is also depicted to be stable in acidic conditions (41) and degraded at a fast rate above pH 6.8. The molecular level of this therapeutic nanodelivery can improve the understanding of this therapeutic nanodelivery system.

CONCLUSION

The TNA nanosystem for delivery of RSV on the neuronal cell line model was successfully studied in this work by promoting the prolonged release activity of the polyphenol compound from the nanocomplex system involving TNA and polymer coating. Future investigations on the molecular level of this nanocomplex on the neuronal cell will give an improved understanding and may promote a new alternative in the treatment of neurological disorder.

ACKNOWLEDGEMENTS

The authors would like to thank Universiti Sains Malaysia for sponsoring this work under research grant; RUI EKSESAIS 2019 (No:1001/CIPPT/8012338).

REFERENCES

1. Dong X. Current strategies for brain drug delivery. Theranostics. 2018;8(6):1481.
2. Kim KT, Lee HS, Lee JJ, Park EK, Lee BS, Lee JY, Bae JS. Nanodelivery systems for overcoming limited transportation of therapeutic molecules through the blood–brain barrier. Future medicinal chemistry. 2018 Nov;10(22):2659-74.
3. Ziental D, Czarczynska-Goslinska B, Mlynarczyk DT, Glowacka-Sobotta A, Stanisz B, Goslinski T, Sobotta L. Titanium dioxide nanoparticles: Prospects and applications in medicine. Nanomaterials. 2020 Feb;10(2):387.
4. Song B, Liu J, Feng X, Wei L, Shao L. A review on potential neurotoxicity of titanium dioxide nanoparticles. Nanoscale research letters. 2015 Dec 1;10(1):342.
5. Jia X, Wang S, Zhou L, Sun L. The potential liver, brain, and embryo toxicity of titanium dioxide nanoparticles on mice. Nanoscale research letters. 2017 Dec 1;12(1):478.
6. Cheng Y, Yang H, Yang Y, Huang J, Wu K, Chen Z, Wang X, Lin C, Lai Y. Progress in TiO 2 nanotube coatings for biomedical applications: a review. Journal of Materials Chemistry B. 2018;6(13):1862-86.
7. Mydin RB, Hazan R, Farid Wajidi MF, Sreekantan S. Titanium dioxide nanotube Arrays for biomedical implant materials and nanomedicine applications. Titanium Dioxide—Material for a Sustainable Environment; Yang, D., Ed. 2018 Jun 27:469-83.
8. Wang Q, Huang JY, Li HQ, Zhao AZ, Wang Y, Zhang KQ, Sun HT, Lai YK. Recent advances on smart TiO_2 nanotube platforms for sustainable drug delivery applications. International Journal of Nanomedicine. 2017;12:151.
9. Graham RM, Hernandez F, Puerta N, De Angulo G, Webster KA, Vanni S. Resveratrol augments ER stress and the cytotoxic effects of glycolytic inhibition in neuroblastoma by downregulating

Akt in a mechanism independent of SIRT1. Experimental & molecular medicine. 2016 Feb;48(2):e210.
10. Chen Y, Tseng SH, Lai HS, Chen WJ. Resveratrol-induced cellular apoptosis and cell cycle arrest in neuroblastoma cells and antitumor effects on neuroblastoma in mice. Surgery. 2004 Jul 1;136(1):57-66.
11. Gatson, J (2019). Use of Resveratrol to Decrease Acute Secondary Brain Injury Following Sports-Related Concussions in Boxers (REPAIR). U.S National Library of Medicine. Published on March 23, 2011. Retrieved July 28, 2020 from https://www.clinicaltrials.gov/ct2/show/NCT01321151
12. Rao YL, Ganaraja B, Joy T, Pai MM, Ullal SD, Murlimanju BV. Neuroprotective effects of resveratrol in Alzheimer's disease. Frontiers in bioscience (Elite edition). 2020 Jan;12:139-49.
13. Moraes DS, Moreira DC, Andrade JM, Santos SH. Sirtuins, brain and cognition: A review of resveratrol effects. IBRO Reports. 2020 Dec 1;9:46-51.
14. Gambini J, Inglῆs M, Olaso G, Lopez-Grueso R, Bonet-Costa V, Gimeno-Mallench L, Mas-Bargues C, Abdelaziz KM, Gomez-Cabrera MC, Vina J, Borras C. Properties of resveratrol: in vitro and in vivo studies about metabolism, bioavailability, and biological effects in animal models and humans. Oxidative medicine and cellular longevity. 2015 Oct;2015.
15. Torres-Hernández YG, Ortega-Díaz GM, Téllez-Jurado L, Castrejyn-Jiménez NS, Altamirano-Torres A, García-Pérez BE, Balmori-Ramírez H. Biological compatibility of a polylactic acid composite reinforced with natural chitosan obtained from shrimp waste. Materials. 2018 Aug;11(8):1465.
16. Xu XL, Zhou GQ, Li XJ, Zhuang XP, Wang W, Cai ZJ, Li MQ, Li HJ. Solution blowing of chitosan/PLA/PEG hydrogel nanofibers for wound dressing. Fibers and Polymers. 2016 Feb 1;17(2):205-11.
17. Hanafy NA, El-Kemary M, Leporatti S. Micelles structure development as a strategy to improve smart cancer therapy. Cancers. 2018 Jul;10(7):238.
18. Kalaycıoğlu Z, Torlak E, Akın-Evingür G, Özen İ, Erim FB. Antimicrobial and physical properties of chitosan films incorporated with turmeric extract. International journal of biological macromolecules. 2017 Aug 1;101:882-8.
19. SMN Mydin RB, Sreekantan S, Hazan R, Farid Wajidi MF, Mat I. Cellular Homeostasis and Antioxidant Response in Epithelial HT29 Cells on Titania Nanotube Arrays Surface. Oxidative medicine and cellular longevity. 2017 Jan 1;2017.
20. Buhrmann C, Yazdi M, Popper B, Kunnumakkara AB, Aggarwal BB, Shakibaei M. Induction of the epithelial-to-Mesenchymal transition of human colorectal Cancer by human TNF-β (Lymphotoxin) and its reversal by resveratrol. Nutrients. 2019 Mar;11(3):704.
21. Kaur G, Willsmore T, Gulati K, Zinonos I, Wang Y, Kurian M, Hay S, Losic D, Evdokiou A. Titanium wire implants with nanotube arrays: a study model for localized cancer treatment. Biomaterials. 2016 Sep 1;101:176-88.
22. Liang C, Wen J, Liao X. A visible-light-controlled platform for prolonged drug release based on Ag-doped TiO_2 nanotubes with a hydrophobic layer. Beilstein Journal of Nanotechnology. 2018 Jun 14;9(1):1793-801.
23. Kumeria T, Mon H, Aw MS, Gulati K, Santos A, Griesser HJ, Losic D. Advanced biopolymer-coated drug-releasing titania nanotubes (TNTs) implants with simultaneously enhanced osteoblast adhesion and antibacterial properties. Colloids and Surfaces B: Biointerfaces. 2015 Jun 1;130:255-63.
24. Mydin RB, Sreekantan S, Hazan R, Qazem EQ, Wajidi MF. Mechanosensitivity response of epithelial HT29 cells on titanium dioxide nanotube array surface via CK8 protein expression. International Journal of Nano and Biomaterials. 2019;8(2):118-28.
25. Sreekantan S, Saharudin KA, Wei LC. Formation of TiO_2 nanotubes via anodisation and potential applications for photocatalysts, biomedical materials, and photoelectrochemical cell. InIOP Conf. Ser.: Mater. Sci. Eng. 2011 Mar (Vol. 21, No. 1, p. 012002).
26. Wang H, Jiang T, Li W, Gao NA, Zhang T. Resveratrol attenuates oxidative damage through activating mitophagy in an in vitro model of Alzheimer's disease. Toxicology letters. 2018 Jan 5;282:100-8.
27. Gupta M, Kaur A. Method development and validation for simultaneous estimation of resveratrol and gallic acid by RP-HPLC. International Journal of Pharmaceutical, Chemical & Biological Sciences. 2019 Jan 1;9(1).
28. Moretyn-Lamas E, Lago-Crespo M, Lage-Yusty MA, Lypez-Hern6ndez J. Comparison of methods for analysis of resveratrol in dietary vegetable supplements. Food chemistry. 2017 Jun 1;224:219-23.
29. Li C, Li Y, Lv H, Li S, Tang K, Zhou W, Yu S, Chen X. The novel anti-neuroblastoma agent PF403, inhibits proliferation and invasion in vitro and in brain xenografts. International Journal of Oncology. 2015 Jul 1;47(1):179-87.
30. Kovalevich J, Langford D. Considerations for the use of SH-SY5Y neuroblastoma cells in neurobiology. InNeuronal cell culture 2013 (pp. 9-21). Humana Press, Totowa, NJ.
31. Van Ginkel PR, Sareen D, Subramanian L, Walker Q, Darjatmoko SR, Lindstrom MJ, Kulkarni A, Albert DM, Polans AS. Resveratrol inhibits tumor growth of human neuroblastoma and mediates apoptosis by directly targeting mitochondria. Clinical Cancer Research. 2007 Sep 1;13(17):5162-9.
32. Salehi B, Mishra AP, Nigam M, Sener B, Kilic M, Sharifi-Rad M, Fokou PV, Martins N, Sharifi-Rad

J. Resveratrol: A double-edged sword in health benefits. Biomedicines. 2018 Sep;6(3):91.
33. Wang T, Weng Z, Liu X, Yeung KW, Pan H, Wu S. Controlled release and biocompatibility of polymer/titania nanotube array system on titanium implants. Bioactive materials. 2017 Mar 1;2(1):44-50.
34. Moseke C, Hage F, Vorndran E, Gbureck U. TiO_2 nanotube arrays deposited on Ti substrate by anodic oxidation and their potential as a long-term drug delivery system for antimicrobial agents. Applied Surface Science. 2012 May 1;258(14):5399-404.
35. Notario-Pérez F, Martín-Illana A, Cazorla-Luna R, Ruiz-Caro R, Bedoya LM, Tamayo A, Rubio J, Veiga MD. Influence of chitosan swelling behaviour on controlled release of tenofovir from mucoadhesive vaginal systems for prevention of sexual transmission of HIV. Marine drugs. 2017 Feb;15(2):50.
36. Hazan R, Sreekantan S, Mydin RB, Abdullah Y, Mat I. Study of TiO_2 nanotubes as an implant application. In AIP Conference Proceedings 2016 Jan 22 (Vol. 1704, No. 1, p. 040009). AIP Publishing LLC.
37. Tosato MG, Vicendo P, Thomas AH, Lorente C. Clearing up the photochemistry of resveratrol: Effect of the solvent. Journal of Photochemistry and Photobiology A: Chemistry. 2018 Dec 1;367:327-31.
38. Arbo BD, André-Miral C, Nasre-Nasser RG, Schimith LE, Santos MG, Costa-Silva D, Muccillo-Baisch AL, Hort MA. Resveratrol Derivatives as Potential Treatments for Alzheimer's and Parkinson's Disease. Frontiers in Aging Neuroscience. 2020 Apr 17;12:103.
39. Andrade S, Ramalho MJ, Pereira MD, Loureiro JA. Resveratrol brain delivery for neurological disorders prevention and treatment. Frontiers in pharmacology. 2018 Nov 20;9:1261.
40. Hanif M, Jabbar F, Sharif S, Abbas G, Farooq A, Aziz M. Halloysite nanotubes as a new drug-delivery system: a review. Clay Minerals. 2016 Jun 1;51(3):469-77.
41. Zupančič, Lavrič Z, Kristl J. Stability and solubility of trans-resveratrol are strongly influenced by pH and temperature. European Journal of Pharmaceutics and Biopharmaceutics. 2015 Jun 1;93:196-204.